

Supplementary Information

Self-assembly of PBTTT-C₁₄ Thin Films in Supercritical Fluids

Nastaran Yousefi,¹ Richard D. Pettipas,² Timothy L. Kelly,² Loren G. Kaake^{1}*

¹Department of Chemistry, Simon Fraser University, 8888 University Dr., Burnaby, BC V5A 1S6, Canada

²Department of Chemistry, University of Saskatchewan, 110 Science Place, Saskatoon, SK S7N 5C9, Canada

Table of Contents

1. Supercritical Fluid Chamber	S2
2. Gravimetric Analysis of PBTTT-C ₁₄ Saturated Solutions	S2
3. Absorption Peak Position Shift as a Function of Temperature	S3
4. Optical Microscopy Images of PBTTT-C ₁₄ Films Grown in SCF and Spin-coated	S4
5. Atomic Force Microscopy Image of Spin-coated PBTTT-C ₁₄	S4
6. GIWAXS Results of PBTTT-C ₁₄ Spin-coated Film	S5
7. Ex-situ UV-vis Absorbance Spectroscopy	S5
8. GIWAXS Results of PBTTT-C ₁₄ Films Grown in SCF	S7
9. Helium Ion Microscopy Images of PBTTT-C ₁₄ Deposited Films	S8
10. References	S8

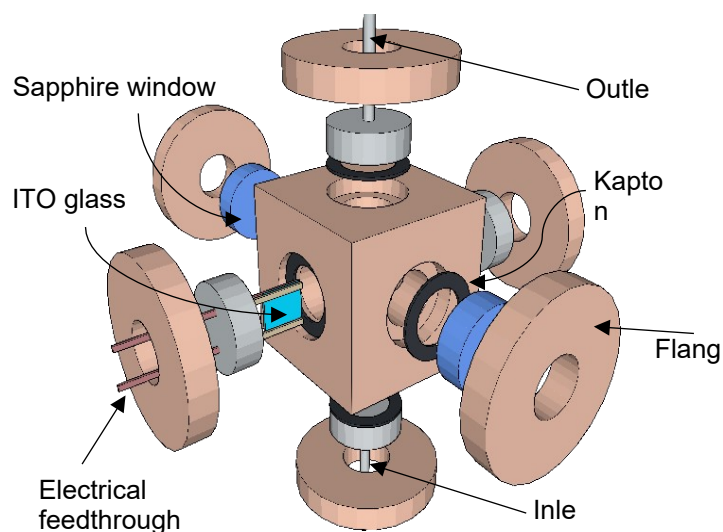


Figure S1. Drawing of pressure chamber and some of its components. Fasteners, heating elements, and mounting elements are omitted for clarity.

1. Supercritical Fluid Chamber

2. Gravimetric Analysis of PBTTT-C₁₄ Saturated Solutions

Gravimetric analysis of PBTTT-C₁₄ saturated solutions was carried out by exhausting the chamber contents through the chamber outlet into a polypropylene vessel. The rapid expansion of the chamber contents cooled the solution below its boiling point, allowing liquid solvent and

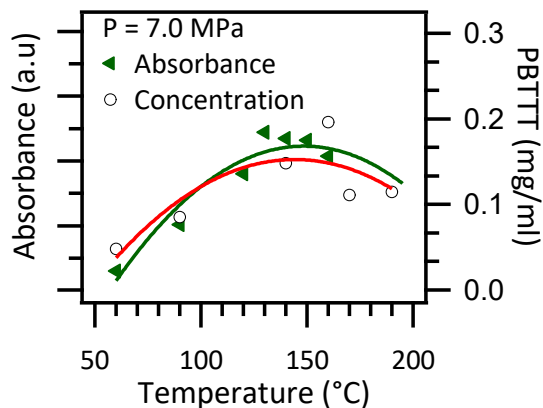


Figure S2. Total integrated absorbance (Left Axis, a.u.) and concentration (Right Axis, mg/ml) as a function of temperature at 7.0 MPa for *n*-pentane: toluene (0.5% mol) system.

(precipitated) PBTTT-C₁₄ to be collected. Solvent was removed from the slurry under reduced pressure, and the dried PBTTT-C₁₄ material was weighed.

3. Absorption Peak Position Shift as a Function of Temperature

We observe that the absorption peak position is a function of temperature, showing a red-shift in the peak maximum for temperatures up to approximately 125 and 100 °C for pure *n*-pentane and *n*-pentane: toluene (0.5% mol) respectively. As the temperature is further increased, a blue-shift is observed for both pure *n*-pentane and *n*-pentane: toluene (0.5% mol) solutions. The absorbance peak center as a function of temperature is calculated by the weighted average of the two Gaussian peaks used to fit the data and the trend in peak position as a function of temperature and pressure can be found in **Figure S3**. The peak shifts toward longer wavelengths with increasing temperature up to a maximum, decreasing with further increases in temperature. The peak shift is a representative of fractionation behavior, where the red-shift of the spectrum is indicating an increase in the conjugation length of the material being dissolved. This is consistent with the solubility behavior of polymers in supercritical fluids, which favors the solvation of low molecular weight and amorphous material.¹⁻⁴ By increasing the temperature further, the polymer solubility diminishes as the longer conjugation length fraction leaving the solution.

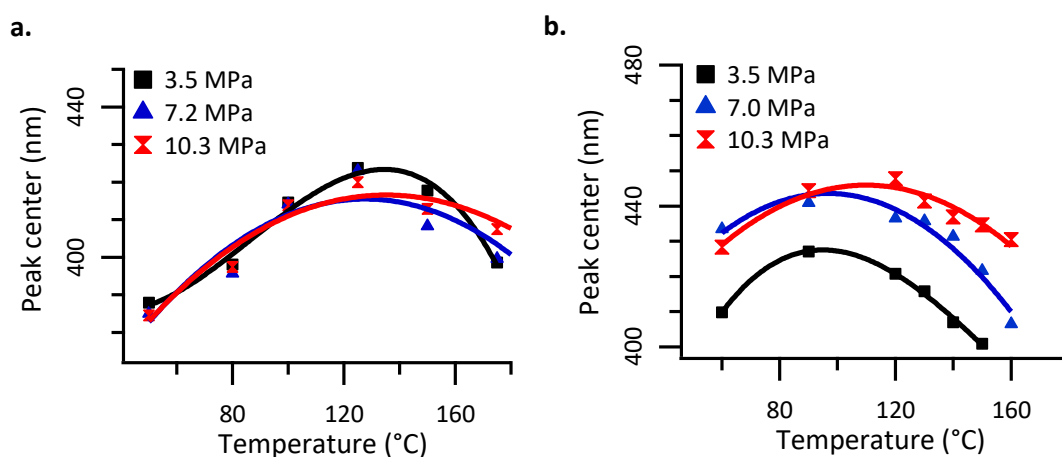


Figure S3. In-situ transmission UV-vis results for the chamber and its content (solution). Estimated center of main absorbance peak as a function of temperature for several pressures for (a) pure *n*-pentane and (b) *n*-pentane: toluene (0.5% mol).

4. Optical Microscopy Images of PBTTT-C₁₄ Films Grown in SCF and Spin-coated

Figure S4 shows the optical microscope images of a series of films grown on resistively heated indium tin oxide (ITO)-coated glass substrates via p-SFD technique. The exposure and saturation in these images have been adjusted to better provide visual confirmation of film deposition and allow the film uniformities to be compared.

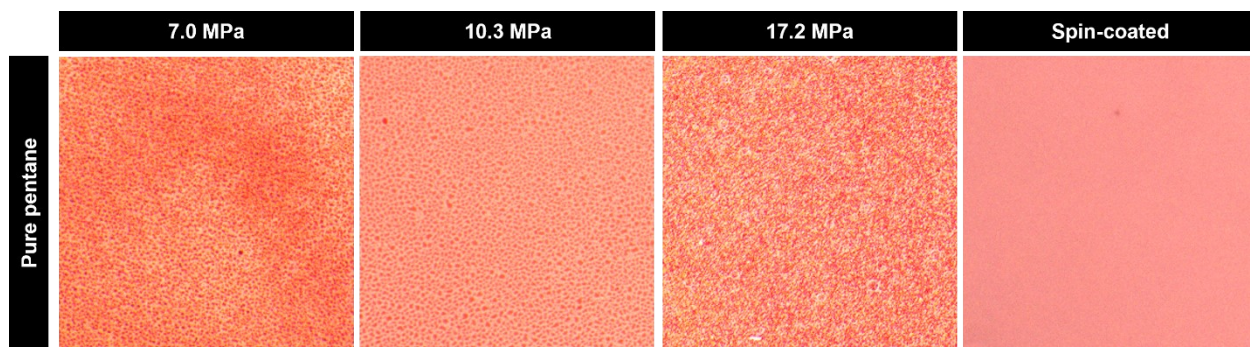


Figure S4. Optical microscopy images of PBTTT-C₁₄ films grown in *n*-pentane at different pressures and spin-coated PBTTT-C₁₄ (with 50x magnification).

5. Atomic Force Microscopy Image of Spin-coated PBTTT-C₁₄

Spin-coated film of PBTTT-C₁₄ was prepared by using 10 mg mL⁻¹ solution in o-dichlorobenzene, and the resulting film thickness was ~30 nm as measured by a Bruker

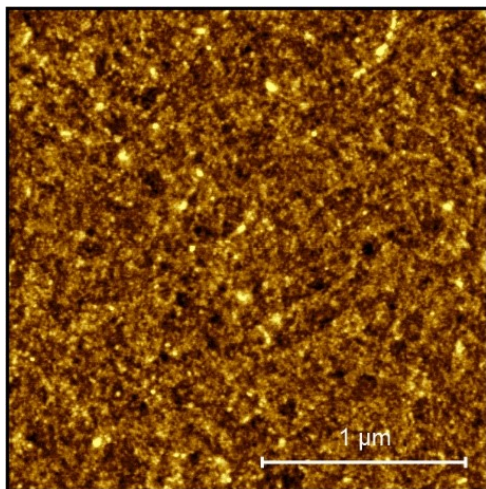


Figure S5. Atomic force microscopy image of PBTTT-C₁₄ film formed via spin-coating.

Dimension Icon atomic force microscope.

6. GIWAXS Results of PBTTT-C₁₄ Spin-coated Film

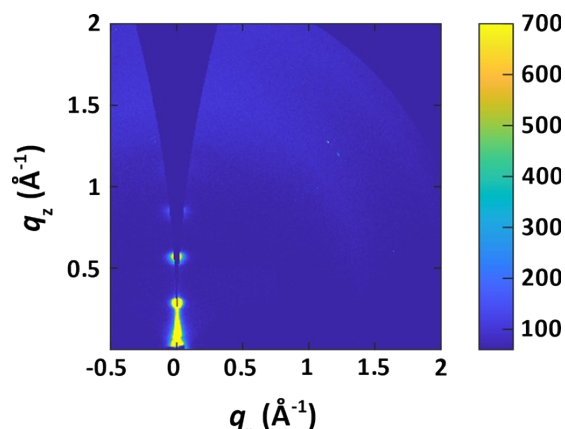


Figure S6. 2D GIWAXS pattern of PBTTT-C₁₄ film formed via spin-coating from 10 mg mL⁻¹ in *o*-dichlorobenzene solution.

7. Ex-situ UV-vis Absorbance Spectroscopy

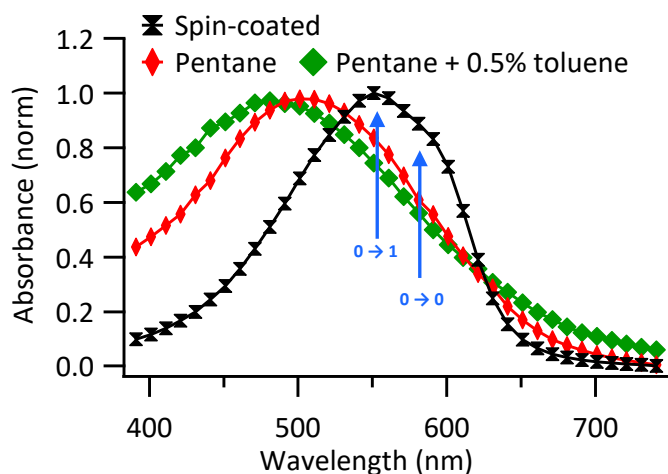


Figure S7. UV-vis spectra measurements taken from the PBTTT-C₁₄ films grown in SCF *n*-pentane and *n*-pentane: toluene (0.5% mol) at 10.3 MPa compared with PBTTT-C₁₄ films formed via spin-coating.

It is common to discuss the extent of aggregation in semiconducting polymer films in terms of the shape of the UV-Vis absorbance spectrum. Specifically, the degree of crystallinity is correlated to the ratio of the first two features in the vibronic progression of the spectrum ($A' = A_{0 \rightarrow 0} / A_{0 \rightarrow 1}$). These structures are the result of a decrease in inhomogeneous broadening,

allowing the fine structure associated with combined vibrational-electronic transitions (a.k.a. the Franck-Condon principle) to become visible. The effect of exciton-exciton coupling modifies the Huang-Rhys factors associated with effect, changing the relative intensities of the fine features in the UV-Vis spectrum. Two types of exciton-exciton coupling typically occur, with J-coupling being resulting from straighter polymer chains and correlated with a spectral redshift. Higher crystallinity also increases interchain interactions, or H-coupling, which is typically associated with spectral blueshift^{5, 6} Based on the UV-vis spectra collected, the films grown via p-SCF have a significantly lower A' values compared to the spin-coated films PBTTT-C₁₄. Given that GIWAX measurements show similar crystallinity in both spin-cast and p-SFD films (**Figures 3 and S6**), the spectral differences observed are likely the result of reduced J-coupling, which is correlated with the sweeping morphologies observed in AFM measurements (**Figure 2**).

8. GIWAXS Results of PBTTT-C₁₄ Films Grown in SCF

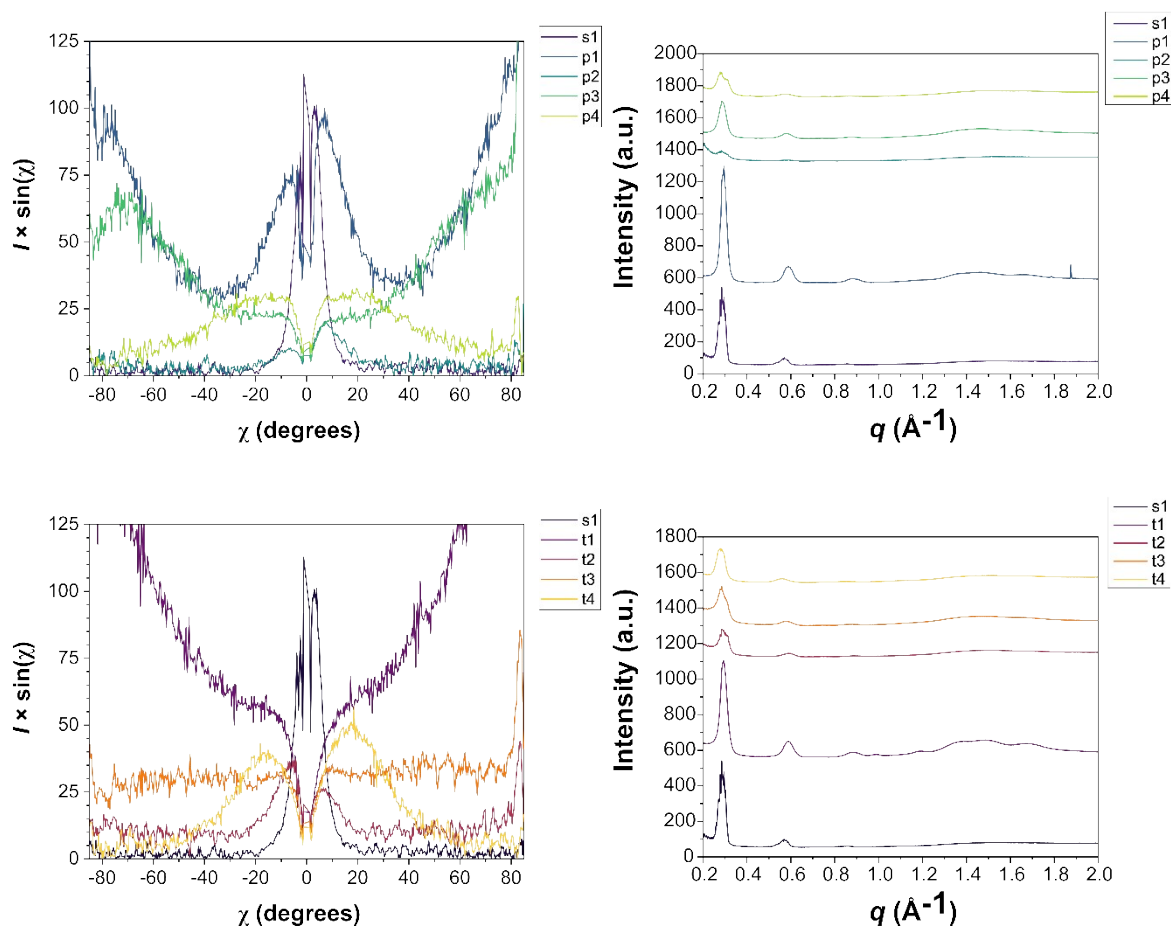


Figure S8. Azimuthal dependence of the corrected scattering intensity for several PBTTT-C₁₄ thin films (left) and their corresponding 1D profiles (right). Samples are labeled as follows: s1 - spin coated, p1 - pentane (P=3.5 MPa), p2 - pentane (7.0 MPa), p3 - pentane (10.3 MPa), p4 - pentane (17.2 MPa), t1 - pentane:toluene (3.5 MPa), t2 - pentane:toluene (7.0 MPa), t3 - pentane:toluene (10.3 MPa), t4 - pentane:toluene (17.2 MPa).

Table S1. The crystalline coherence length (CCL) of the (100) reflection calculated using the Scherrer equation.

	S1	P1	P2	P3	P4	T1	T2	T3	T4
FWHM (Å ⁻¹)	0.03	0.029	0.035	0.039	0.054	0.034	0.045	0.044	0.046
*CCL (nm)	19	19	16	14	10	17	13	13	12

*Instrumental broadening was not subtracted from the FWHM in the analysis.

9. Helium Ion Microscopy Images of PBTTT-C₁₄ Deposited Films

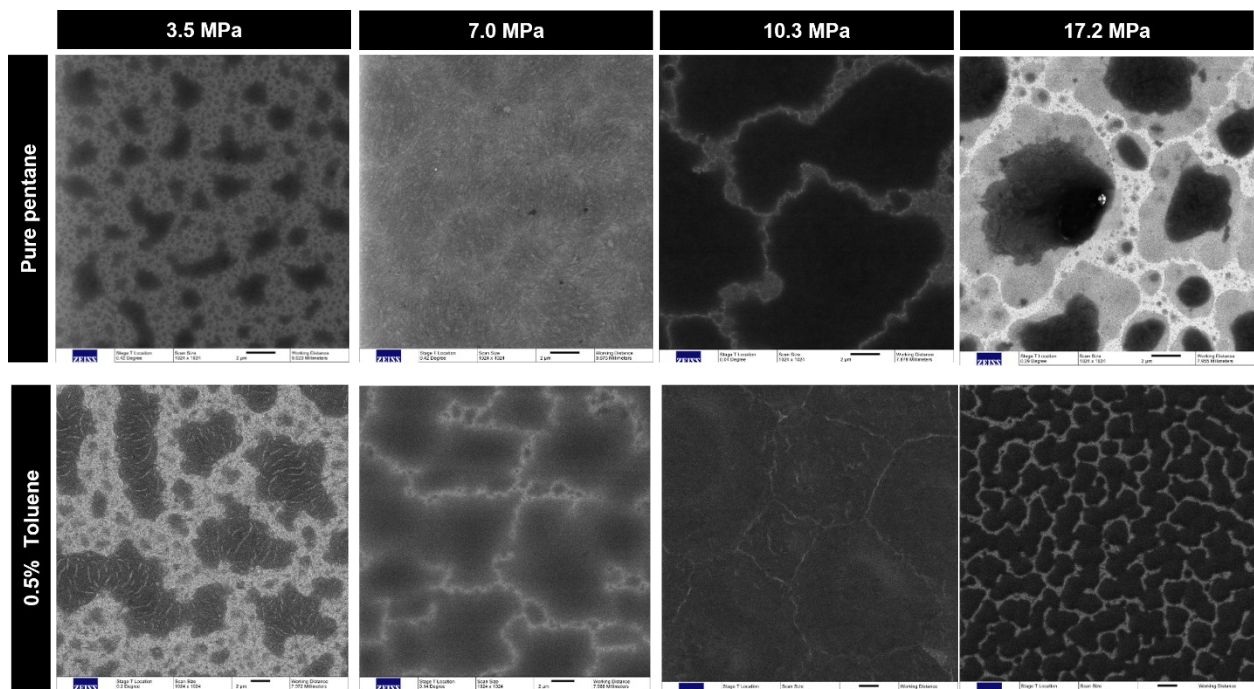


Figure S9. Helium ion microscopy images of PBTTT-C₁₄ films grown in pure *n*-pentane and *n*-pentane: toluene (0.5% mol) at different pressures. The scale bar is 2 μ m.

10. References

1. J. M. Desimone, Z. Guan and C. S. Elsbernd, *Science*, 1992, **257**, 945-947.
2. Y. T. Shieh, J. H. Su, G. Manivannan, P. H. C. Lee, S. P. Sawan and W. D. Spall, *J. Appl. Polym. Sci.*, 1996, **59**, 707-717.
3. Y. T. Shieh, J. H. Su, G. Manivannan, P. H. C. Lee, S. P. Sawan and W. D. Spall, *J. Appl. Polym. Sci.*, 1996, **59**, 695-705.
4. Hunter, E.; Richards, R. B. *U.S. Pat.*, 1948.
5. F. C. Spano, *J. Chem. Phys.*, 2005, **122**, 234701-234701.
6. J. Clark, C. Silva, R. H. Friend and F. C. Spano, *Phys. Rev. Lett.*, 2007, **98**, 206406-206406.